DOUBLY FED INDUCTION GENERATOR SYSTEMS for Wind Turbines

BY S. MÜLLER,
M. DEICKE,
& RIK W.
DE DONCKER

A viable alternative to ADJUST SPEED over a wide range at MINIMAL COST

THE AIM OF WIND TURBINE SYSTEMS DEVELOPMENT is to continuously increase output power. A few years ago, the rated output power of production-type units reached 200 kW. By 1999, the average output power of new installations climbed to 600 kW. The largest series production units today are specified to deliver 1.5-MW output power (Table 1). It is anticipated that in the near future, power rating of wind turbines will increase further, especially in offshore applications. For example, the prototype of a Nordex N80 with a rated power of 2.5 MW was installed in March 2000 near Aachen.

Many low-power wind turbines built to-date were constructed according to the "Danish concept" (Fig. 1), in which wind energy is transformed into electrical energy using a simple squirrel-cage induction machine directly connected to a three-phase power grid. The rotor of the wind turbine is coupled to the generator shaft with a fixed-ratio gearbox. Some induction generators use pole-adjustable winding configurations to enable operation at different synchronous speeds. However, at

©COURTESY OF ENRON WIND GMBH

1077-2618/02/$17.00©2002 IEEE

any given operating point, this Danish turbine basically has to operate at constant speed.

The construction and performance of fixed-speed wind turbines very much depends on the characteristics of mechanical subcircuits, e.g., pitch control time constants, main breaker maximum switching rate, etc. The response time of some of these mechanical circuits may be in the range of tens of milliseconds. As a result, each time a gust of wind hits the turbine, a fast and strong variation of electrical output power can be observed. These load variations not only require a stiff power grid to enable stable operation, but also require a sturdy mechanical design to absorb high mechanical stresses. This strategy leads to expensive mechanical construction, especially at high-rated power.

TABLE 1. WIND POWER STATIONS CURRENTLY IN OPERATION WITH RATED POWER ABOVE 1.0 MW [1]

Manufacturer/ Type	*Nominal Power in (kW)*	*Rotor Control*	*Speed Control*	*Rotor Diameter (m)*
DeWind D6	1,250	Pitch	Variable	64
AN BONUS	2,000	CombiStall	Const	76
Nordex N80	2,500	Pitch	Variable	80
Enron EW1.5s	1,500	Pitch	Variable	70
Enercon E-66	1,800	Pitch	Variable	70
Enron EW3.6	3,600	Pitch	Variable	100
Pro&Pro MD70	1,500	Pitch	Variable	70
Vestas V80	2,000	Pitch	Variable	80

Adjustable Speed Generators

Modern high-power wind turbines are capable of adjustable speed operation. Key advantages of adjustable speed generators (ASGs) compared to fixed-speed generators (FSGs) are:

- They are cost effective and provide simple pitch control; the controlling speed of the generator (frequency) allows the pitch control time constants to become longer, reducing pitch control complexity and peak power requirements. At lower wind speed, the pitch angle is usually fixed. Pitch angle control is performed only to limit maximum output power at high wind speed.
- They reduce mechanical stresses; gusts of wind can be absorbed, i.e., energy is stored in the mechanical inertia of the turbine, creating an "elasticity" that reduces torque pulsations.
- They dynamically compensate for torque and power pulsations caused by back pressure of the tower. This back pressure causes noticeable torque pulsations at a rate equal to the turbine rotor speed times the number of rotor wings.
- They improve power quality; torque pulsations can be reduced due to the elasticity of the wind turbine system. This eliminates electrical power variations, i.e., less flicker.
- They improve system efficiency; turbine speed is adjusted as a function of wind speed to maximize output power. Operation at the maximum power point can be realized over a wide power range. Fig. 2 illustrates typical output power-speed curves as a function of turbine speed and wind speed. As a result, energy efficiency improvement up to 10% is possible (Fig. 3).
- They reduce acoustic noise, because low-speed operation is possible at low power conditions.

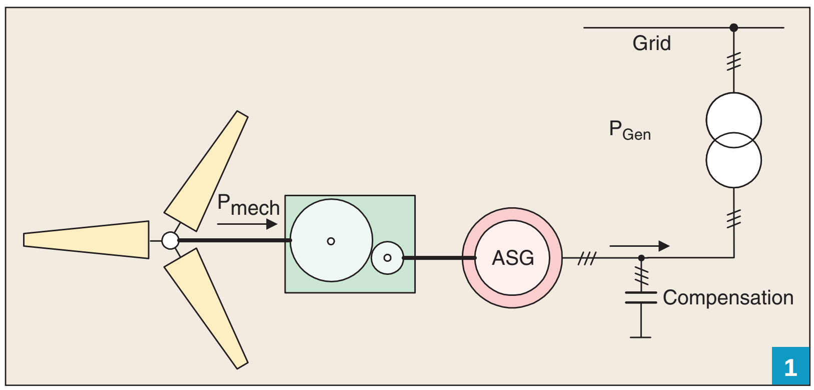

Fixed speed "Danish" concept.

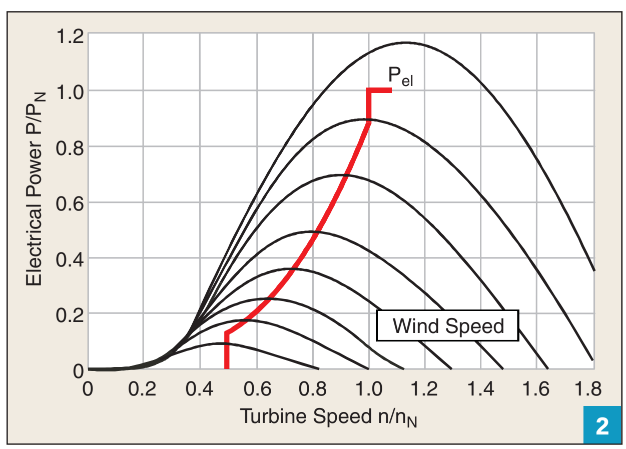

Electrical output power as a function of turbine speed. Parameter curves are plotted for different wind speeds. Maximum power point tracking (red curve) can be realized with a speed variable system.

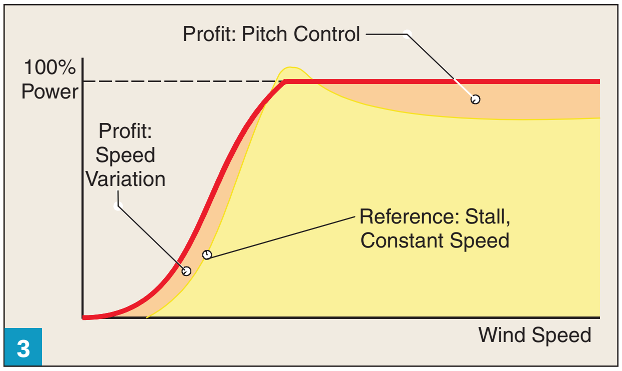

Efficiency gains due to adjustable speed wind turbines.

In addition, most ASG-based wind turbines can offer island-operation capability. Island operation is difficult to realize with the Danish concept.

Direct-in-Line ASG System

One possible implementation scheme of ASGs is shown in Fig. 4. A synchronous generator is used to produce variable-frequency ac power. A power converter connected in series with the ASG transforms this variable-frequency ac power into fixed-frequency ac power. Although these direct-in-line systems have been built up to 1.5 MW, several disadvantages are apparent:

- The power converter, which has to be rated at 1 p.u. total system power, is expensive.
- Inverter output filters and EMI filters are rated for 1 p.u. output power, making filter design difficult and costly.
- Converter efficiency plays an important factor in total system efficiency over the entire operating range.

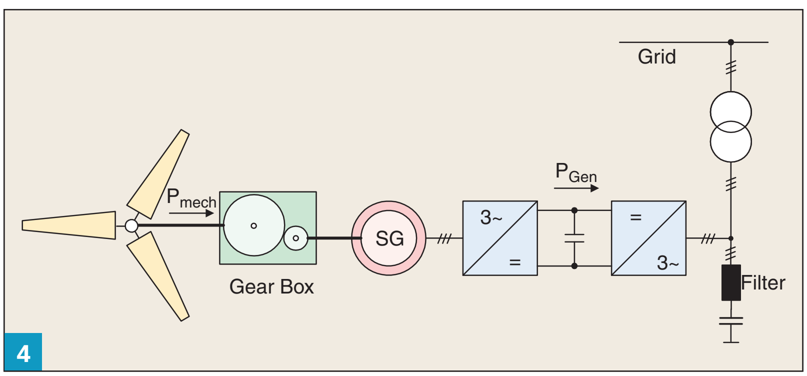

Direct-in-line wind turbine system.

Doubly Fed Induction Generator ASG System

Recent developments seek to avoid most disadvantages of direct-in-line converter based ASGs. Fig. 5 shows an alternative ASG concept that consists of a doubly fed induction generator (DFIG) with a four-quadrant ac-to-ac converter based on insulated gate bipolar transistors (IGBTs) connected to the rotor windings. Compared to direct-in-line systems, this DFIG offers the following advantages:

- Reduced inverter cost, because inverter rating is typically 25% of total system power, while the speed range of the ASG is ±33% around the synchronus speed (Fig. 6).
- Reduced cost of the inverter filters and EMI filters, becuase filters are rated for 0.25 p.u. total system power, and inverter harmonics represent a smaller fraction of total system harmonics.
- Improved system efficiency; Table 2 shows the system losses for different windmill concepts. The losses are shown separately for the generator and for the IGBT inverters. Approximately 2-3% efficiency improvement can be obtained.
- Power-factor control can be implemented at lower cost, because the DFIG system (four-quadrant converter and induction machine) basically operates similar to a synchronous generator. The converter has to provide only excitation energy.

In addition, compared to silicon-controlled rectifier (SCR) based Kramer drives [3], the DFIG with a four-quadrant converter in the rotor circuit enables decoupled control of active and reactive power of the generator.

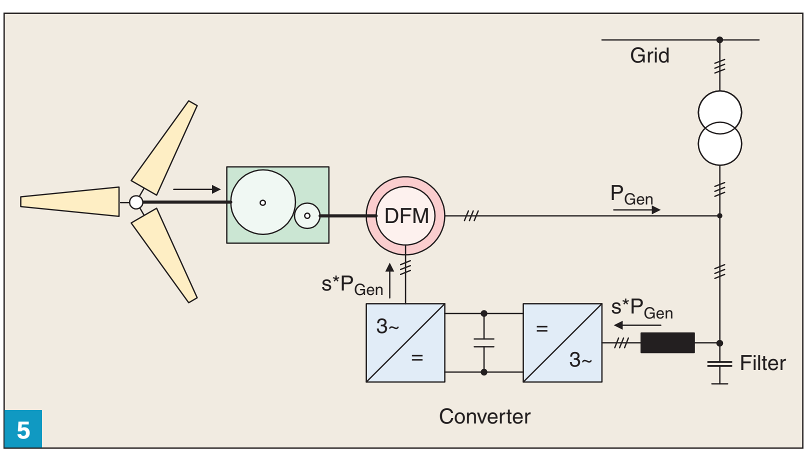

Doubly fed induction generator wind turbine system.

Dynamic Model of a Doubly Fed Induction Generator

To develop decoupled control of active and reactive power, a DFIG dynamic model is needed. The construction of a DFIG is similar to a wound rotor induction machine (IM) and comprises a three-phase stator winding and a three-phase rotor winding. The latter is fed via slip rings. The voltage and torque equations of the DFIG in a stationary reference frame are:

$$v_{Sj} = r_S \cdot i_{Sj} + \frac{\partial \psi_{Sj}}{dt} \qquad j = \{1,2,3\} \tag{1}$$

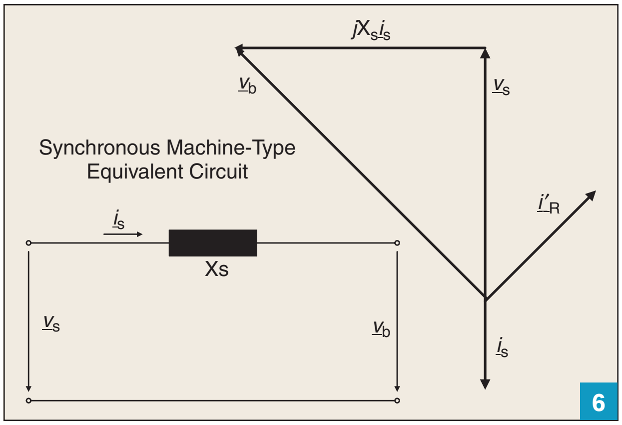

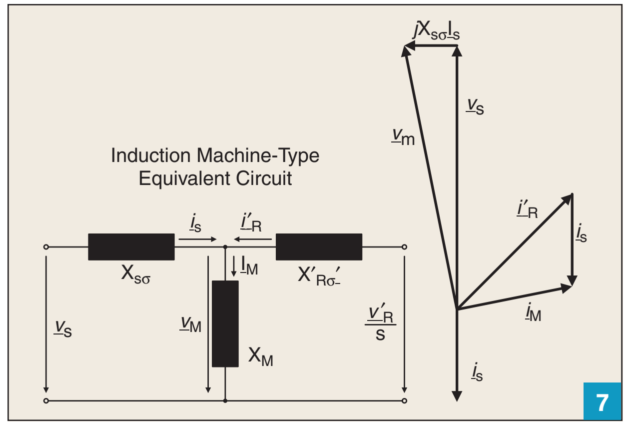

Maximum output power as a function of slip *s* (left) or speed ratio n/n_0 (right).

Equivalent circuit and vector diagram of the (synchronous) DFIG.

$$v'_{Rj} = r'_R \cdot i'_{Rj} + \frac{\partial \psi_{Rj}}{dt} \qquad j = \{1,2,3\} \tag{2}$$

$$T_{el} = \frac{p}{2} \cdot \sum_{j=1}^{3} i_j \cdot \frac{d\psi_j}{d\vartheta}. \tag{3}$$

In these equations, all quantities are referred to the stator, i.e., transformed rotor quantities (superscript ′) are used. Transforming these equations from three-phase to two-phase components and subsequently rotating all variables into a synchronous reference frame (dq) according to

$$v_d = \frac{2}{3} \cdot \left[\begin{array}{l} v_1 \cdot \cos\vartheta + v_2 \cdot \cos\left(\vartheta - \frac{2\cdot\pi}{3}\right) \\ + v_3 \cdot \cos\left(\vartheta + \frac{2\cdot\pi}{3}\right) \end{array} \right] \tag{4}$$

$$v_d = \frac{2}{3} \cdot \left[\begin{array}{l} -v_1 \cdot \sin\vartheta - v_2 \cdot \sin\left(\vartheta - \frac{2\cdot\pi}{3}\right) \\ -v_3 \cdot \sin\left(\vartheta + \frac{2\cdot\pi}{3}\right) \end{array} \right] \tag{5}$$

yields

$$\underline{v} = v_d + j \cdot v_q \tag{6}$$

$$\underline{v}_S = r_S \cdot \underline{i}_S + \frac{\partial \underline{\psi}_S}{dt} + j \cdot \omega_S \cdot \underline{\psi}_S \tag{7}$$

$$\underline{v}'_R = r'_R \cdot \underline{i}'_R + \frac{\partial \underline{\psi}'_R}{dt} + j \cdot \omega_R \cdot \underline{\psi}'_R \tag{8}$$

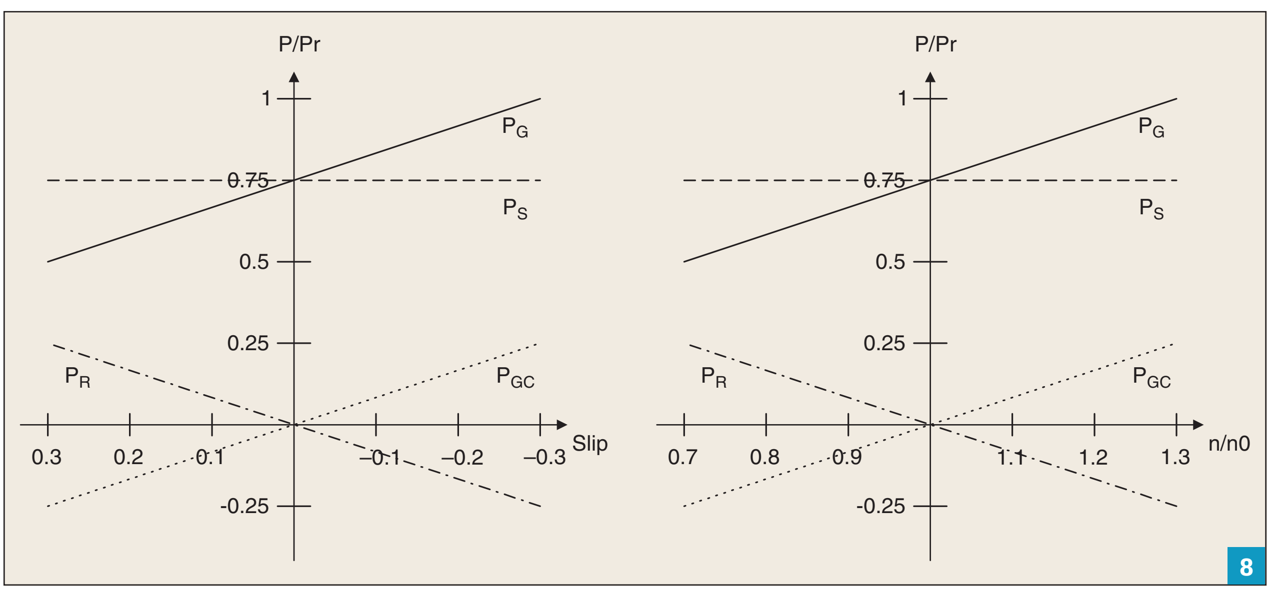

Induction machine type equivalent circuit and vector diagram of the DFIG.

$$\underline{\psi}_S = L_S \cdot \underline{i}_S + L_m \cdot \underline{i}'_R \tag{9}$$

$$\underline{\psi}_R = L_m \cdot \underline{i}_S + L_R \cdot \underline{i}'_R \tag{10}$$

$$T_{el} = -\frac{3}{2} \cdot p \cdot \mathrm{Im}\left\{\underline{\psi}_S \cdot \underline{i}_S{}^*\right\}, \tag{11}$$

with $\omega_R = \omega_S - \omega_{\text{mech}}$, the rotor slip frequency.

The synchronous reference frame can be linked to the stator or rotor flux of the machine. However, a reference frame linked to the stator voltage space vector $\underline{v}_S$ is a convenient alternative because the DFIG operates as a generator maintaining or being fed with constant stator voltage [4]. Hence, stator voltage and stator current are either given (line operation) or controlled (island operation) variables.

Two interpretations of the DFIG dynamic equations are possible, depending on the state variables selected in the model. A synchronous machine model is obtained when selecting the flux linked to the rotor currents [or back-electromotive force (EMF) voltage] as a state variable. Selecting the air-gap flux (or magnetizing current) as a state variable invariably leads to an induction machine type model. This can be demonstrated easily for steady state. Both models give valuable insights on how the DFIG works and can be controlled.

In steady-state and neglecting-stator resistance, the stator voltage (7) reduces to

$$\underline{V}_S = j \cdot \omega_S \cdot L_S \underline{I}_S + \underline{V}_b \tag{12}$$

$$\underline{V}_b = j \cdot \omega_S \cdot L_m \underline{I}'_R . \tag{13}$$

In (13), voltage vector $\underline{V}_b$ represents the back-EMF voltage induced in the stator by rotor current $\underline{I}_{R'}$. This rotor current can be considered as the field current of the (synchronous) DFIG. The associated DFIG steady-state equivalent circuit and vector diagram are shown in Fig. 7.

By selecting the magnetizing current as a state variable, the next steady-state equivalent circuit and vector diagram can be found (Fig. 8).

In this induction machine-type equivalent circuit, a slip s can be introduced, according to

$$s = \frac{\omega_S - \omega_{\text{mech}}}{\omega_S} = \frac{\omega_R}{\omega_S}. \tag{14}$$

TABLE 2. COMPARISON OF LOSSES OF DIFFERENT TURBINE SYSTEMS

	Generator	Inverter
Danish Concept	Cannot be constructed economically, due to mechanical reasons.	
Direct Line	ca. 3.5 %	ca. 3 %
DFIG	ca. 3.5%	ca. 0.75%

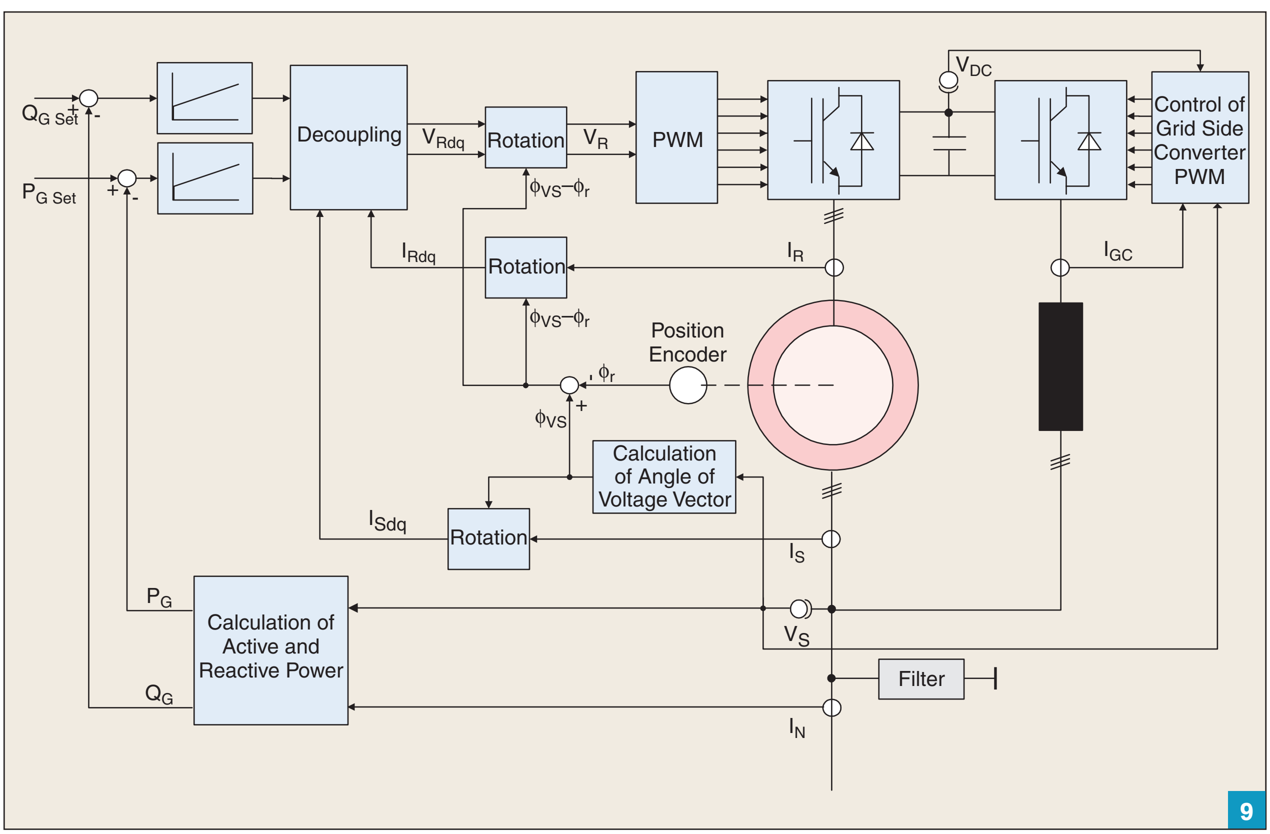

Vector controller block diagram for DFIG.

Neglecting rotor resistance and rotor leakage inductance, one can derive that the rotor voltage amplitude equals

$$V_R \approx s * a_{SR} * V_S , \quad (15)$$

with a_{SR}, the voltage-transformation ratio between stator and rotor. This ratio is selected such that the voltage rating of the four-quadrant converter matches the stator voltage at maximum speed to avoid transformers in the rotor circuit.

IT IS ANTICIPATED THAT THE POWER RATING OF WIND TURBINES WILL INCREASE.

The active power delivered to the rotor by the four-quadrant converter and the mechanical power delivered to the shaft of the generator can be calculated according to the well-known IM equations

$$P_R = s * P_S \quad (16)$$

$$P_{\text{mech}} = (1 - s) * P_S . \quad (17)$$

Both (14) and (15) clearly describe the power flow in the DFIG for over-synchronous and under-synchronous operation. Above synchronous speed, the four-quadrant converter operates as a generator of active power delivering power to the grid parallel to the DFIG. Below synchronous speed, the four-quadrant converter circulates (bypasses) active power from the grid into the rotor circuit. Fig. 6 illustrates these relationships.

DFIG Vector Control

To guarantee stable operation and enable independent control of active and reactive power of the DFIG, a model-based feed-forward controller is developed using the dynamic model equations mentioned above. A block diagram is shown in Fig. 9. Fundamentally, the proposed controller is a vector controller, because the synchronous reference frame in which the machine equations are described is linked to the stator voltage space vector $\underline{v}_s$ and not to the stator or rotor flux vector, as is common in field-oriented controllers for drives.

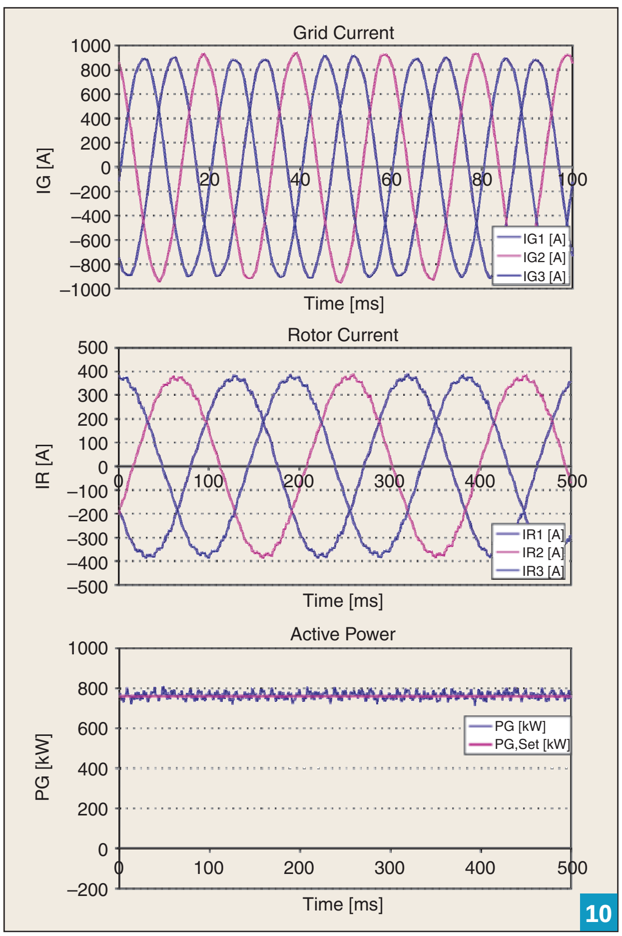

DFIG ac line current (top), rotor current (middle), output active power command and instantaneous active power (bottom).

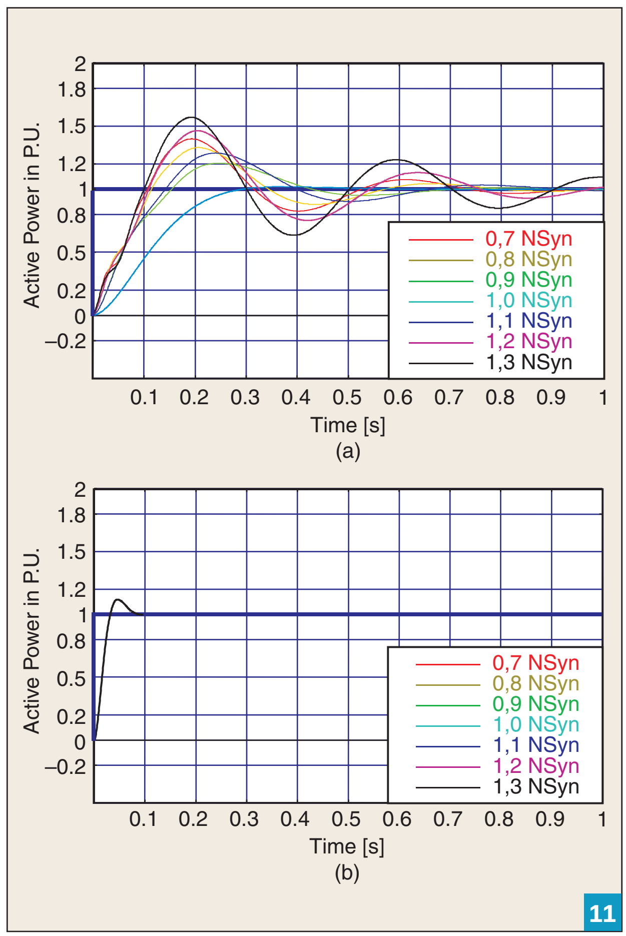

Transient active power step response of DFIG. (a) Response without decoupling at different speeds. (b) Response with decoupling.

All measured quantities, i.e., stator and rotor current $\underline{i}_S$ and $\underline{i}_R$, are transformed into the synchronous reference frame. A decoupling circuit calculates from the desired active and reactive power signals the rotor voltage command v_{Rd} and v_{Rq}. A reverse vector rotation computes magnitude and phase of the rotor voltage command in a stationary reference frame. Furthermore, the measured rotor current signals are used for rotor current regulation to minimize the effects of parameter detuning and inverter gain errors.

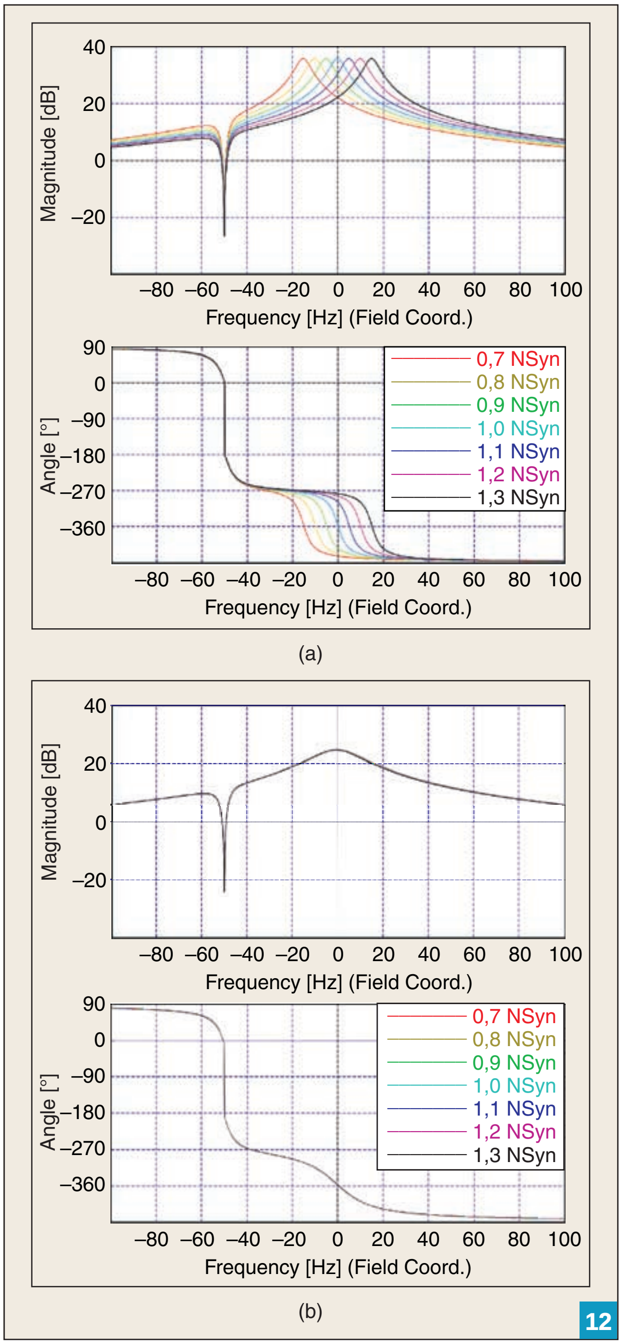

Bode diagram of the rotor voltage to stator current $\underline{I}_S/\underline{V}_R$ admittance. (a) Admittance $\underline{I}_S/\underline{V}_R$ Bode plots without decoupling. (b) Admittance $\underline{I}_S/\underline{V}_R$ Bode plots with decoupling.

Simulation Results

Detailed system simulations were performed to evaluate the performance of the vector-controlled doubly fed generator. Fig. 10 illustrates the DFIG line current, rotor current, and output active power. Notice the low THD content in the line current of the DFIG system.

To analyze system response and tune feedback parameters, an active power step response is simulated. Fig. 11(a) shows the response when the decoupling network is inactive, i.e., the machine is controlled using the basic steady-state voltage model based on slip control. Note that system performance depends on speed due to the coupling between d and q variables. Fig. 11(b) shows system response when decoupling is performed according to the dy-

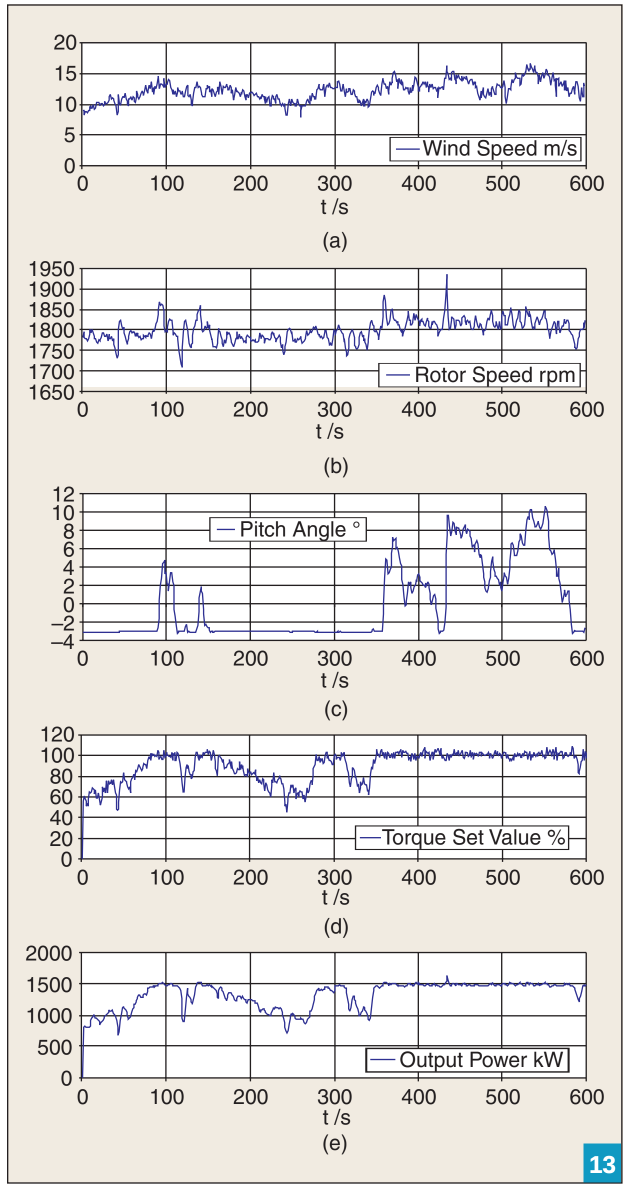

Recorded waveforms on a 1.5 MW DFIG system. (a) Wind speed. (b) DFIG rotor speed. (c) Pitch angle of turbine blades. (d) DFIG controller output power command. (e) DFIG measured output power.

namic model of the DFIG. The system's response is quick and speed invariant.

The same performance improvement can be noticed in the frequency domain. Small signal Bode plots for the $\underline{I}_S / \underline{V}_R{}^*$ transfer function (admittance) are shown in Fig. 12 [(a) for slip control and (b) for decoupled operation].

The 3-dB bandwidth reaches ±20 Hz when decoupled control is turned on. Note that a positive frequency indicates a rotation of the superimposed small signal space vectors in the direction of the fundamental component, i.e., at a frequency above 50 Hz. A negative frequency indicates a small signal analysis with a frequency below 50 Hz. One can notice that the slip controlled DFIG has a strong dependency on speed.

Experimental Results

Measurements were made on a wind turbine system having a doubly fed Concycle generator produced by SEG, Germany. The rated power is 1.5 MW, and the rated speed is n_r=1,800 rpm. Typical results are illustrated in Fig. 13. The top trace shows variation of wind speed as a function of time (elapsed time 0-600 s). Fig. 13(b) shows generator speed.

The main turbine controller aims at controlling speed using pitch control [Fig. 13(c)]. Up to the time instant t=350 s, the pitch control is not very active because maximum power is not reached. Hence, the main controller seeks to maximize output power according to the maximum efficiency curve shown in Fig. 4. Beyond 350 s, one can see wind speed going up to approximately 15 m/s. Fig. 13(d) shows that the wind turbine controller now limits the torque command at 100%. The actual output power delivered to the grid is shown in Fig. 13(e) and matches the command value perfectly.

Notice that in this constant, maximum power mode, the pitch controller sets the blades to keep speed within bounds. At the time instance t=450 s, the elasticity of the variable-speed DFIG wind turbine system is demonstrated. For a short while, wind speed rapidly reaches 17 m/s. The pitch controller is not capable of following this fast gust of wind. Hence, the speed of the turbine blades is allowed to increase storing energy into the turbine's inertia. During this transient, output power remains practically constant, avoiding power surges into the power grid.

Summary

This article shows that adjustable speed generators for wind turbines are necessary when output power becomes higher than 1 MW. The doubly fed induction generator system presented in this article offers many advantages to reduce cost and has the potential to be built economically at power levels above 1.5 MW, e.g., for off-shore applications.

A dynamic model of the DFIG was derived to develop a vector controller to decouple dynamically active and reactive power control. Simulations show excellent response of the DFIG independent of speed. Measurements obtained from 1.5 MW units currently in operation confirm the theoretical results.

Acknowledgment

The authors would like to thank Tacke Windenergie, Salzbergen, Germany, for the measurements shown in Fig. 13.

References

[1] Windenergie (2001) [Online]. Available: http://www.wind-energie.de/informationen/informationen.htm

[2] Q.N. Ph, *Praxis der feldorientierten Drehstromantriebs-regelung.* Expert Verlag, 1993.

[3] R.W. De Doncker, "AC-AC power converters," in *Wiley Encyclopedia of Electrical and Electronics Engineering*, J. Webster, Ed. New York: Wiley, 1999, vol. 1, pp. 13-25.

[4] T. Jahns and R.W. De Doncker, "Control of generators," in *The Control Handbook*, W. Levins, Ed. Boca Raton, FL: CRC, 1996.

[5] D. Arsudis, "Doppeltgespeister Drehstromgenerator mit Spannungszwischenkres-Umrichter im Rotorkreis für Windkraftanlagen," Ph.D. dissertation, Fakultät für Maschinenbau und Elektrotechnik Technische Universität Braunschweig, Germany, 1989.

[6] H. Späth, *Steuerverfahren für Drehstrommaschinen: Theoretische Grundlagen.* Berlin, Germany: Springer-Verlag, 1983.

[7] H. Stemmler and A. Omlin, "Converter controlled fixed-frequency variable-speed motor/generator," presented at the IPEC '95, Japan.

[8] E. Bogalecka, "Dynamics of the power control of double fed induction generator connected to the soft grid," in *Proc. IEEE Int. Symp. Ind. Electron.*, Budapest, 1993, pp. 509-513.

[9] H.K.. Lauw, C.H. Weigand, and D.A. Marckx, "Variable-speed wind system design: Final Report," U.S. Dept. of Energy, Washington, DC, Rep. DOE/BP/99893-TI, 1993.

S. Müller (s.mueller@newage-avkseg.com) and M. Deicke are with SEG GmbH & Co. in Kempen Germany. Rik W. De Doncker is with the Institute for Power Electronics and Electrical Drives in Aachen Germany. Deicke is a Member of the IEEE, and De Doncker is a Senior Member of the IEEE. This article first appeared in its original format at the 2000 IEEE/IAS Annual Meeting.